

# Fiber Bragg grating hydrophone with high sensitivity

Wentao Zhang (张文涛), Yuliang Liu (刘育梁), and Fang Li (李芳)

Optoelectronic System Laboratory, Institute of Semiconductors, Chinese Academy of Sciences, Beijing 100083

Received January 28, 2008

A fiber Bragg grating (FBG) hydrophone with high sensitivity was demonstrated. This hydrophone used a rubber diaphragm and a copper hard core as the sensing element. To compensate the hydrostatic pressure, a capillary tube was fixed at the end of the hydrophone. Theoretical analysis of the acoustic pressure sensitivity was given in this letter. Experiments were carried out to test the frequency response of the hydrophone. The result shows that when the Young's modulus of the diaphragm is higher, a flatter frequency response will be obtained.

OCIS codes: 060.2370, 230.1480, 060.4230.

doi: 10.3788/COL20080609.0631.

The fiber optic hydrophone has been one of the most promising acoustic detection devices in future operational sonar systems due to its high sensitivity, wide dynamic range, immunity to electromagnetic interference (EMI), and feasibility in multiplexing<sup>[1]</sup>. Many conventional fiber hydrophones are based on Mach-Zehnder interferometer (MZI) or Michelson interferometer, which include a sensing arm and a reference arm. The fiber is usually wound on a plastic cylinder. However, the multiplexing of the interferometric fiber hydrophones is complex<sup>[2]</sup>, and the dimensions of this type of hydrophone cannot be very small<sup>[3]</sup>. So, fiber Bragg grating (FBG) hydrophones become popular for use in under water acoustic detection<sup>[4–6]</sup>. In the past several years, many configurations for FBG hydrophones and pressure sensors have been demonstrated. These include bare FBG<sup>[4,5]</sup>, polymer coating on bare FBG<sup>[6]</sup>, and shielded polymer coating of FBG<sup>[7]</sup>. Such correction methods are likely to work better if the dimensions are reduced while the sensitivity is enhanced. In this letter, we reported a FBG hydrophone with high sensitivity that uses a thin metal cylinder and a diaphragm<sup>[8]</sup>. Owing to the greater deformation of the diaphragm with a hard core in the center, thin dimensions and an ultra high sensitivity have been achieved.

The proposed FBG hydrophone is shown in Fig. 1. The water went into the hydrophone from the sensing hole and filled the inside cavity of the hydrophone. Then the acoustic pressure could act on the surface of the rubber diaphragms to induce axial strain in the FBG. A hard core, which was made of copper, was affixed at the center of each diaphragm to enhance the sensitivity and fix the fiber. Two capillaries were fixed on the covers at the both ends of the hydrophone, which were used to balance the inside and outside hydrostatic pressure. When the

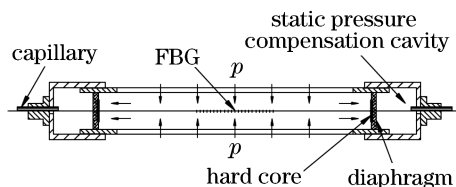


Fig. 1. Schematic of the hydrophone.

hydrophone operated in the deep water, the hydrostatic pressure would induce large deformation of the diaphragms to break the fiber if the static pressure was not compensated. Several assumptions and design considerations should be stated before the analysis. The operating range was restricted to small displacements so that the linear elasticity theory could be used and only low frequencies (100–1000 Hz) were considered to avoid dealing with acoustic scattering. The static pressure sensitivity was assumed to be equal to the dynamic pressure sensitivity<sup>[9,10]</sup>, so that we could use static mechanics analysis. Because the Young's moduli of the sensor shell and the hard core (132 GPa) are much higher than that of the rubber (less than 0.1 GPa), and the acoustic pressure we measured is always less than 1 kPa, we only considered the deflection of the rubber diaphragm. Finally, the FBG was considered to be perfectly fixed to the rubber diaphragm.

Having stated the assumptions, the sensitivity of the hydrophone can be given as<sup>[8]</sup>

$$\frac{\Delta\lambda_B}{\lambda_B \cdot p} = \frac{(1 - p_e) \frac{R^4}{64D} \left( 1 - \left(\frac{r}{R}\right)^4 + 4 \left(\frac{r}{R}\right)^2 \ln \frac{r}{R} \right)}{\frac{L}{2} + \frac{AE_f R^2}{16\pi D} \left[ 1 - \left(\frac{r}{R}\right)^2 \frac{1 - \left(\frac{r}{R}\right)^2 + 4 \ln^2 \left(\frac{r}{R}\right)}{1 - \left(\frac{r}{R}\right)^2} \right]}, \quad (1)$$

where  $\lambda_B$  is the center wavelength of the FBG,  $\Delta\lambda_B$  is the center wavelength shift of the FBG,  $p$  is acoustic pressure, and

$$D = \frac{Et^3}{12(1 - \mu^2)}, \quad (2)$$

$R$  is the radius of the diaphragm,  $t$  is the thickness of the diaphragm,  $r$  is the radius of the hard core,  $E$  is the Young's modulus of the diaphragm,  $\mu$  is the Poisson's ratio,  $A$  is the cross section area of the fiber,  $E_f$  is the Young's modulus of the fiber,  $L$  is the fixed length of the FBG, and  $p_e = 0.22$  is the effective photo-elastic constant of the fiber.

Two types of hydrophones were fabricated and tested. Commercially available FBGs were used with a reflective wavelength of about 1527 nm. The used Young's moduli of the polyurethane rubber, T-805 and EU 2500, are 17 and 70 MPa, respectively. The outer radius of the metal

**Table 1. Parameters Used in the Configuration**

Parameter	Value	Parameter	Value
$L$ (cm)	8	$r$ (mm)	1.2
$t$ (mm)	1	$\mu$	0.3
$A$ (mm <sup>2</sup> )	0.0123	$E_f$ (GPa)	72
$R$ (mm)	3.5	$\lambda_B$ (nm)	1527

cylinder is 5 mm and the radius of the hard core is about 1.2 mm. Other parameters of the hydrophones are shown in Table 1.

A standard piezoelectric (PZT) hydrophone and the fiber optic hydrophone were put into the water tank together. The acoustic source on the other side of the water tank was fed by a frequency generator. The PZT hydrophone and the fiber optic hydrophone were placed 5 cm apart, which is very close compared with the minimum acoustic wavelength of 1.5 m. The size of the water tank is smaller than half of the acoustic wavelength in the water. Thus, we considered the local acoustic pressure of the two hydrophones to be the same when they were placed close to each other. The PZT hydrophone was used to measure the local acoustic pressure.

Figure 2 shows the schematic of the demodulation system for a single hydrophone. The network was illuminated by an amplified spontaneous emission (ASE) light source with a 40-nm bandwidth (1520 – 1560 nm). The commercially available FBG used in our configuration has a center wavelength of 1527 nm, a peak power reflectivity of  $\sim 60\%$ , and a spectral bandwidth of  $\sim 0.12$  nm. The light reflected from the FBG became the light source of the unbalanced MZI. The optical path difference (OPD) of the unbalanced MZI is 7 mm. A PZT fiber stretcher in one of the MZI arms in the demodulator was used to induce a phase-shift carrier signal on the sensor output signals to enable passive recovery of dynamic phase-shift information using phase generated carrier (PGC) demodulation<sup>[11]</sup>. The test was performed in the frequency range from 100 to 1000 Hz. The frequency response of the hydrophone was shown in Fig. 3.

Ideally, the frequency response should be flat, however as Fig. 3 showed, the frequency response varied across the measured bandwidth. This variation was the mechanical resonance of the rubber diaphragm and the hard core. But Fig. 3 demonstrates that when the Young's modulus is higher, the frequency response will be flatter. Because when the Young's modulus was lower, the viscoelasticity of the polymer would become more

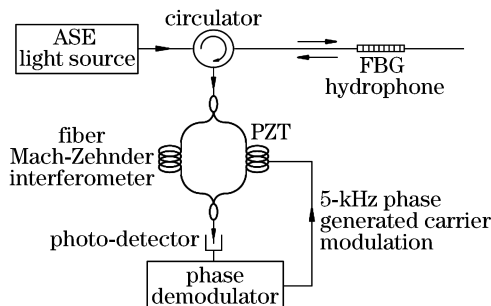


Fig. 2. Schematic of the demodulation system.

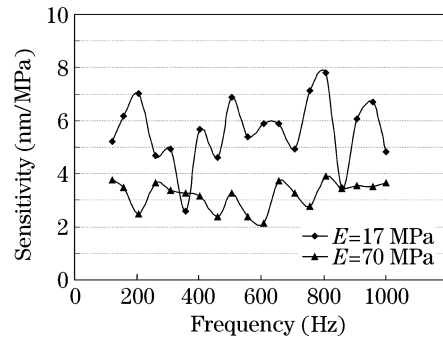


Fig. 3. Frequency response of the hydrophone.

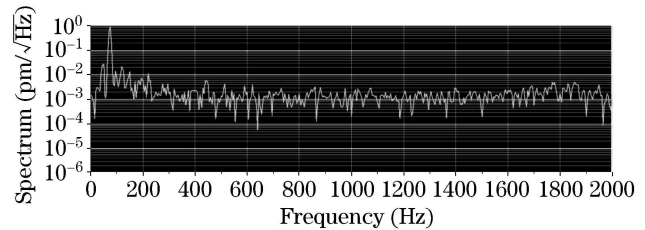


Fig. 4. Demodulation result of the FBG hydrophone.

significant and the natural frequency of the sound-induced vibration modes of the diaphragm would become lower<sup>[12]</sup>. A balance should be found between the sensitivity and the frequency response, which requires further investigation.

Figure 4 is the demodulated signal of the FBG hydrophone in frequency domain when the input acoustic signal is 73 Hz. This figure shows that the noise floor of the hydrophone is about  $10^{-3}$  pm/ $\sqrt{\text{Hz}}$  for 7-mm OPD of MZI at 1 kHz. For practical applications, the hydrophone sensitivity goal is the level of the acoustic background noise of the quiet ocean, which is called deep-sea state zero (DSS0). At 1 kHz, the DSS0 level is  $100 \mu\text{Pa}/\sqrt{\text{Hz}}$ . In our configuration, a sensitivity of about 6 nm/MPa was achieved (Fig. 3), which resulted in a minimum detectable acoustic signal of  $170 \text{ mPa}/\sqrt{\text{Hz}}$  at 1 kHz. This sensitivity is approximately 100 times higher than that measured with a conventional coated FBG<sup>[6]</sup>. This level of detection is three orders higher than the current PZT hydrophones and the target noise floor of DSS0. However, because the presented structure greatly enhanced the wavelength-to-pressure sensitivity, we believe that the target noise floor of DSS0 could be achieved by replacing the FBG with a distributed feedback (DFB) fiber laser to reduce the noise floor of the hydrophone<sup>[13]</sup>.

We have shown a novel technique for enhancing the pressure sensitivity of a FBG hydrophone using a diaphragm with a hard core in the center. By optimizing these two parameters, a pressure sensitivity of 6 nm/MPa has been achieved when the radius of the hard core is 1.2 mm and the outer radius of the hydrophone is 5 mm. The in-water acoustic test showed the frequency response of the two types of hydrophones. We found that when the Young's modulus of the diaphragm is higher, a flatter frequency response will be obtained. Because of its thin dimensions, this hydrophone is expected to be used in

the towed hydrophone arrays.

This work was supported by the Key Projects Program of Chinese Academy of Sciences under Grant No. CXJJ-177. The authors also wish to thank Yuanhui Liu for his help with the experiment. W. Zhang's e-mail address is zhangwt@semi.ac.cn.

## References

1. P. Nash, IEE Proc.-Radar Sonar Navig. **143**, 204 (1996).
2. G. A. Cranch, P. J. Nash, and C. K. Kirkendall, IEEE Sensor. J. **3**, 19 (2003).
3. J. A. Bucaro, B. H. Houston, and E. G. Williams, J. Acoust. Soc. Am. **89**, 451 (1991).
4. N. E. Fisher, D. J. Webb, C. N. Pannell, D. A. Jackson, L. R. Gavrilov, J. W. Hand, L. Zhang, and I. Bennion, Appl. Opt. **37**, 8120 (1998).
5. N. Takahashi, K. Yoshimura, S. Takahashi, and K. Imamura, Ultrasonics **38**, 581 (2000).
6. D. J. Hill and G. A. Cranch, Electron. Lett. **35**, 1268 (1999).
7. H.-J. Sheng, M.-Y. Fu, T.-C. Chen, W.-F. Liu, and S.-S. Bor, IEEE Photon. Technol. Lett. **16**, 1146 (2004).
8. W. Zhang, L. Liu, F. Li, and Y. Liu, Chin. Opt. Lett. **5**, 507 (2007).
9. G. B. Hocker, Appl. Opt. **18**, 3679 (1979).
10. R. Hughes and J. Jarzynski, Appl. Opt. **19**, 98 (1980).
11. A. Dandridge, A. B. Tveten, and T. G. Giallorenzi, IEEE J. Quantum Electron. **18**, 1647 (1982).
12. A. W. Leissa, *Vibration of Plates* (US Government Printing Office, Washington D. C., 1969).
13. D. J. Hill, B. Hodder, J. De Freitas, S. D. Thomas, and L. Hickey, Proc. SPIE **5855**, 904 (2005).